Modelling Dynamic Aerosol Processes for Indoor Ultrafine Particles

Donghyun Rim[1], Lance Wallace[1], Andrew Persily[1], and Jung-il Choi[2*]

[1]National Institute of Standards and Technology.
[2]Yonsei University, South Korea

[*]*Corresponding email: jic@yonsei.ac.kr*

SUMMARY

This study has investigated aerosol transformation processes for four common sources of indoor ultrafine particles (UFP): gas stove, electric stove, candle, and hair dryer. For each of the four UFP sources, the temporal change in particle size distribution (3 nm to 100 nm) was measured during particle decay. An analytical model was developed based on the discrete general dynamic mass-balance equation considering coagulation, deposition, and ventilation. The results indicate that in addition to particle deposition and ventilation loss, coagulation is a dominant physical process for changes in indoor UFP size distributions. Especially at high UFP concentrations, coagulation was found to be a dominant process that transforms small particles to larger sizes in a short time.

IMPLICATIONS

It is important to understand how indoor UFP concentrations and size distributions vary for different indoor sources. This study developed a particle dynamics model that analyzes differential effects of coagulation, deposition, and ventilation for indoor UFP.

KEYWORDS

Indoor aerosol, Ultrafine particles, Coagulation, Deposition, Aerosol Process

INTRODUCTION

The UFP emissions from indoor sources are intermittent but often much stronger than outdoor sources (He et al. 2004; Wallace 2006). Following emission into an occupied space, UFPs may experience aerosol processes such as coagulation and condensation (Wallace et al. 2008). In indoor environments, UFP loss mechanisms such as deposition and ventilation play an important role in particle size distribution. Considerable work has been done in the past decade in modeling indoor particle dynamics considering particle emission and deposition, even though only few studies have experimentally measured the deposition rates of UFPs. Fewer researchers (Ito and Harashima 2011, Colman and Nazaroff 2008) have investigated the coagulation of indoor UFPs, since it is quite challenging to simultaneously track the separate effects of coagulation, deposition and ventilation. Also, earlier studies have not been able to track particles much lower than 10 nm in diameter due to instrument limitations; in our studies we have been able to measure particles as small as 3 nm and have also discovered that some processes such as cooking with gas and electric stoves and using power tools emit >90 % of the particles in the < 10 nm range. The objective of this study is to investigate the coagulation of indoor UFPs from combustion and consumer products. Using continuous monitoring of size-resolved UFPs in conjunction with an analytical modeling of particle dynamics, the present study examines the coagulation and deposition of indoor UFPs.

METHODS

Experimental Measurements

This study used experimental measurements and analytical modeling to investigate the dynamics of the indoor UFP size distributions. Experimental measurements were conducted in a full scale test house, which consists of three bedrooms, two baths, kitchen, and dining and living area. The total floor area and volume of the house are 140 m^2 and 340 m^3, respectively.

In the test house, particle monitoring tests were conducted from January 2007 to September 2010. These studies monitored size-resolved UFP concentration due to four different indoor sources: gas stove, electric stove, candle, and hair dryer. The particles were generated in the kitchen with the gas and electric stoves, while they are generated in the master bedroom with the candle and hair dryer. The particle sources were turned on for 10 min to 20 min; the subsequent particle decay was monitored and the dynamical model was applied to the decay period. The particles from each source were monitored in the master bedroom using a scanning mobility particle sizer (SMPS) (Model 3936, TSI, St. Paul, MN), which consists of an electrostatic classifier (Model 3080), a nano-DMA (Model 3085) and a water-based condensation particle counter (CPC; Model 3786). This system monitored particles ranging from 2 nm to 100 nm using a sheath flow rate of 15 L/s and 6 L/s with 10:1 sheath/aerosol flow ratio. It was extremely important to ensure that inlet sheath flow is laminar and accurately regulated, and precisely matches the exhaust flow. As small flow disturbances can result in decreased resolutions, aerosol flow rates were measured before and after each experiment using a bubble flow rate meter. At least three measurements were taken and all three were required to be within 3 % of the desired flow rate. The sampling rate of UFPs was set at 2.5 min: 2 min of measurement and 30 s for the voltage to return to baseline. Based on the measurement efficiency curve for the water-based CPC, the minimum measurable particle size was 2 nm. In this study, a stronger radiation source (3080N electrostatic classifier, TSI, Shoreview, MN) was used to improve the charging efficiency for the smallest particles. The uncertainty of measuring particle number concentration was estimated to be 12 % based on combining the individual uncertainties of flow rate, particle charge distribution, voltage adjustment, and particle charge efficiency in quadrature.

In this study, two different sets of particle deposition rates were used depending on the fan operation mode. For the candle and hair dryer tests that were performed with the central furnace fan off, the deposition rates analytically derived from Lai-Nazaroff model (2001) were used. The rates are from 0.01 h^{-1} to 2.5 h^{-1} for particles sizes going down from 200 nm to 2 nm. The tests with the gas/electric stoves were conducted with the central fan recirculating approximately 6 house volumes of air per hour. In this case, the deposition rate (k) is a composite of at least three processes: deposition to interior surfaces in the house; capture on the furnace filter; and deposition to ductwork during the period of the central fan running. Using the measured values of size-resolved deposition rates for the range from 8 nm to 100 nm, (Rim et al. 2010), a linear logarithmic relationship for particle size and deposition rate was estimated as follows and employed to estimate deposition rates for the smaller particles from 2 nm to 8 nm and the larger particles from 100 nm to 200 nm:

$$\ln(k) = -0.752\ln(d_p) + \ln(9.67) \qquad \text{Equation (1)}$$

This relationship yielded the deposition rates ranging from 0.18 h^{-1} to 5.7 h^{-1} for particles sizes from 200 nm to 2 nm. A detailed description of this analysis is described in the previous study (Rim et al. 2010).

Analytical Model

Aerosol particle dynamic behavior was analyzed with an indoor aerosol model that considered coagulation, deposition, and ventilation in a single, well-mixed air volume. Effects of condensation and evaporation were not considered, even though particle condensation caused increases in particle mass in some tests. Due to this effect, conservation of particle mass was checked and data affected by condensation and evaporation was excluded from the analysis. The governing equation for the model is as follows.

$$\frac{\partial n(v,t)}{\partial t} = \frac{1}{2}\int_0^v \beta_{v-\bar{v}} n(v-\bar{v},t) n(\bar{v},t) d\bar{v} - n(v,t)\int_0^\infty \beta_{v,\bar{v}} n(\bar{v},t) d\bar{v} - (k+a) n(v,t) \quad \text{Equation (2)}$$

where $n(v,t)$[m^{-3}] is the particle number concentration for particle volumes [m^3] between □ and $v+dv$ at time t [s]; □−□ and □ are volumes of two coagulating particles; v is the volume of newly coagulated particle; β is the coagulation kernel (collision kernel). a is the air change rate [h^{-1}]; and, k is the particle deposition rate [h^{-1}].

The first two terms on the right hand side in Equation (2) represent the particle gain and loss due to coagulation in which two particles collide and stick together. The third term represents the particle loss due to deposition and ventilation. In the present study, Equation (2) is solved by using the semi-implicit procedure in Jacobson (2005) with a volume fraction factor (f) in order to preserve volume concentrations of the particles. A volume concentration ($\rho_{k,t}$) for size bin k can be written as

$$\rho_{k,t} = \frac{\rho_{k,t-\Delta t} + \Delta t \sum_{j=1}^{k} \sum_{i=1}^{k-1} f_{i,j,k} \beta_{i,j} \rho_{i,t} n_{j,t-\Delta t}}{1 + \Delta t \sum_{j=1}^{N_B} (1 - f_{k,j,k}) \beta_{k,j} n_{j,t-\Delta t}} \quad \text{Equation (3)}$$

where Δt is a time step, N_B is total number of size bins, and $f_{i,j,k}$ is the volume fraction factor defined as

$$f_{i,j,k} = \begin{cases} \dfrac{v_{k+1} - V_{i,j}}{v_{k+1} - v_k} \dfrac{v_k}{V_{i,j}}, & v_k \le V_{i,j} \le v_{k+1},\ k < N_B \\ 1 - f_{i,j,k-1}, & v_{k-1} \le V_{i,j} \le v_k,\ k > 1 \\ 1, & V_{i,j} \ge v_k, \quad k = N_B \\ 0, & \text{otherwise} \end{cases} \quad \text{Equation (4)}$$

where $V_{i,j} = v_i + v_j$ is an intermediate volume between particle size bins i and j.

The coagulation kernel (β) can account for Brownian motion, convective Brownian enhancement, gravitational sedimentation, turbulent inertial motion, turbulent shear, van der Waals forces, and fractal geometry. The details for calculating the coagulation kernel are described in Jacobson (2005). In the present study, we tested three coagulation models that

consider 1) Brownian motion [Brownian]; 2) Brownian motion + van der Waals and viscous forces [VDW]; and 3) Brownian motion + van der Waals and viscous forces + fractal geometry [Fractal24] (particles > 24 nm can be particle aggregates). For each of the three models, the study tested three values of the Hamaker constant: 20, 100, and 200. The Hamaker constant is an empirical value that varies with particle composition. In general, it is low for organic particles and high for metal particles. The analytical model was used to find a model and Hamaker constant most closely matching the observed evolution of the size distributions resulting from the four sources.

RESULTS

Figure 1 shows coagulation kernels for collisions of any two particles between 2nm and 64 nm. In the graph, the x-axis and y-axis represent the diameters of the particles. The contour values represent the collision rate between the two particles. The figure indicates that the collision rate is largest for a small particle colliding with a large particle. Also, the rate increases for the particles larger than 24 nm when those particles are considered as fractal (Figure 1b).

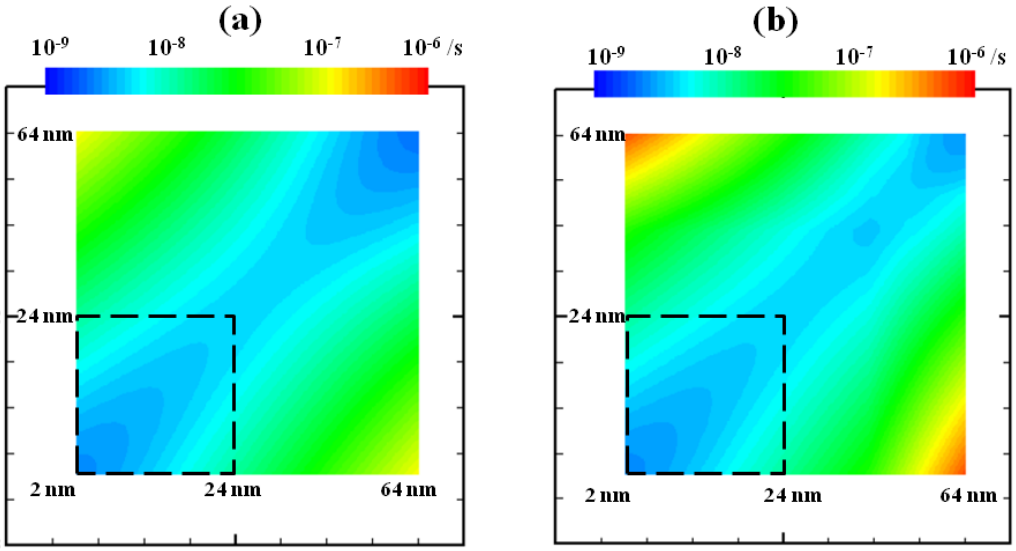

Figure 1. Coagulation kernel for two cases: (a) Brownian motion + van der Waals (b) Brownian motion + van der Waals + Fractal (>24 nm)

Using the calculated coagulation kernel, the model predicted the evolution of the particle size distribution over the first 20 minutes of the decay period. Figure 2a and 2b illustrate the change in particle size distribution with time for two indoor sources: gas stove and candle. The figures show that the analytical model can predict the general pattern of UFP size distribution, i.e., decreasing particle number and increasing geometric mean diameter with time. The model fit is better with higher particle concentrations, in which case coagulation is more important than deposition and ventilation. The model fit becomes less accurate as the number concentrations are reduced. This decrease in accuracy can be explained by the reduced coagulation effect and increased errors due to well-mixed assumption and local air flow effect.

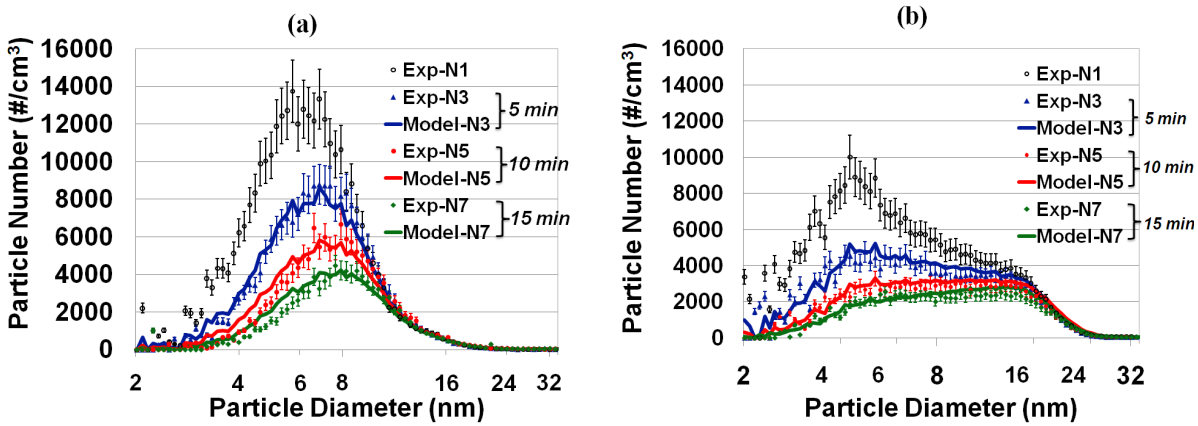

Figure 2. Examples of the analytical model fittings: (a) gas stove, (b) candle burning. The error bar represents 12 % measurement error. The numerals (N1, N3…) refer to the scans following the beginning of the decay period.

DISCUSSION

Table 1 summarizes the UFP size distribution and the best coagulation model/Hamaker constant for the four tested indoor sources. The table indicates that the particle peak occurs between 4 nm and 9 nm for the gas stove, electric stove, and candle, while the peak is larger than 14 nm for hair dryer.

Table 1. Summary of the analytical model results

Source Tested	Test ID	Peak Conc. (10^3/cm^3)	Geometric Mean Diameter (nm)	Best model(s)	Best-fitting Hamaker Const.	Avg. (SD) Root Mean Square (RMS)[a]
Gas Stove	GAS1	321	5.7	Brownian+VDW + Fractal24 [b]	20	364 (78)
	GAS2	294	5.5	Brownian+VDW	20	339 (70)
	GAS3	238	7.1	Brownian+VDW	100	153 (52)
Electric Stove	ELEC1	92	8.8	Brownian+VDW (+Fractal24) [c]	200	148 (21)
	ELEC2	24	4.8	Brownian+VDW	20-200[d]	88 (15)
	ELEC3	177	7.4	Brownian+VDW (+Fractal24)	200	194 (127)
Candle	CAND1	318	4.3	Brownian+VDW + Fractal24	100	359 (115)
	CAND2	61	6.6	Brownian+VDW (+Fractal24)	20 or 100	122 (30)
	CAND3	190	4.5	Brownian+VDW (+Fractal24)	100	262 (49)
Hair Dryer	HAIR1	208	14	Brownian+VDW + Fractal24	200	166 (27)
	HAIR2	456	22	Brownian+VDW + Fractal24	100	289 (62)
	HAIR3	375	22	Brownian+VDW + Fractal24	100	654 (186)

a. The mean (SD) RMS difference in particle number between the measurement and model prediction are based on the fittings of eight consecutive particle size distributions with an interval of 2.5 minutes during the decay period.
b. Brownian+ van der Waals +Fractal (>24nm)
c. (+Fractal24) represents that considering a fractal of 24 nm in the model has minimal effect on the model results.
d. This indicates that there was no big difference in the model result when varying Hamaker constant from 20 to 200.

The results suggest that the Brownian and van der Waals forces are important in modeling indoor particle coagulation. The fractal effect seems to be significant for one of the gas stove tests and for the hair dryer test. However, it seems that with low concentrations (ELEC1, ELEC2, and CAND2), considering fractal geometry in the model does not improve the model prediction. The best fitting Hamaker constant varies with the source. For gas stove and candle, a value between 20 and 100 produces optimal fit to the experimental data, while a constant between 100 or 200 is more appropriate for electric stove and hair dryer. This result implies that particles from gas stove and candle likely consist of organic matter and that those from electric stove and hair dryer are metal particles. Further studies of particle sampling and imaging technique can be used to investigate more details. When the particle concentration is low and the coagulation effect is small (ELEC2), varying the Hamaker constant makes small differences in the model accuracy and it seems difficult to find the best-fitting Hamaker constant.

CONCLUSIONS

Coagulation was usually the dominant process affecting particle dynamics; in some cases deposition was also important. Air change rates were minor effects. Coagulation models that consider Brownian, van der Waals force and fractal geometry can predict with reasonable accuracy the temporal particle size distribution for several indoor sources: hair dryer, candle, and gas/electric stove. Using appropriate coagulation parameters and deposition rate is required for an accurate prediction of indoor UFP dynamics.

REFERENCES

Coleman B.K., Lunden M.M., Destaillats H. et al. 2008. Secondary organic aerosol from ozone-initiated reactions with terpene-rich household products. *Atmos. Environ.* 42, 8234-8245.

He C., Morawska L., Hitchins J. et al. 2004. Contribution from indoor sources to particle number and mass concentrations in residential houses. *Atmos. Environ.* 38, 3405-3415.

Ito K., Harashima, H. 2011. Coupled CFD analysis of size distributions on indoor secondary organic aerosol derived from ozone/limonene reactions. *Building Environ.* 46, 711-718

Jacobson M.Z. 2005. *Fundamentals of Atmospheric Modeling*. Cambridge: Cambridge University Press.

Rim, D., Wallace, L., Persily A. 2010. Infiltration of outdoor ultrafine particles into a test house. *Environ. Sci. Technol. 44,* 5908–5913.

Wallace, L. 2006. Indoor Sources of Ultrafine and Accumulation Mode Particles: Size Distributions, Size-Resolved Concentrations, and Source Strengths, *Aerosol Sci. Technol.* 40(5), 348-360.